172. A Case Study of Kinematical, Microphysical, and Lightning Characteristics of a Tornadic Supercell

MILIND SHARMA[a]*, ROBIN TANAMACHI[a], ERIC BRUNING[b], KRISTIN CALHOUN[c], HOWARD BLUESTEIN[d], JANA HOUSER[e], JEFFREY SNYDER[c], ZACHARY WIENHOFF[d]

[a]*Purdue University,* [b]*Texas Tech University,* [c]*NOAA National Severe Storms Laboratory,* [d]*University of Oklahoma,* [e]*Ohio University*

1. Introduction

Previous studies have shown that a combination of radar and lightning observations can be effective in diagnosing the dynamics and electrification processes of thunderstorms (Bruning et al. 2007; Tessendorf et al. 2007; Deierling and Petersen 2008; Wiens et al. 2008; Bruning et al. 2010; Emersic et al. 2011; Calhoun et al. 2013, 2014).

Stolzenburg et al. (1998a,b,c) improved conceptual understanding of the variation of electric fields within and outside of the main updraft regions of different types of convective thunderstorms. They found that mesoscale convective storms (MCS), isolated supercells, and mountain storms around New Mexico shared common electrical structures. The convective updraft regions had four charge regions of alternate polarity, with the lowest region being positive. On the other hand, convective regions outside the updraft were found to possess at least six distinct charge regions with alternating polarity. The main positive and negative regions were found within the upper and middle levels, respectively, with weaker charge regions near the base and top of clouds. However, there were considerable differences between heights and temperatures at which the charge regions were found in updrafts. These observations illustrated the complexity of electric structure of thunderstorms and the limits of classic tripole model of thunderstorms (Williams 1989).

Rust and MacGorman (2002) demonstrated that there exist 'inverted polarity' storms with their main positive charge region at middle levels and the main negative charge region confined to the upper levels in the thunderstorms. This 'anomalous' charge structure deviated from earlier observations and led to many studies which focused on the diagnostic differences between the normal and anomalous charge structures in thunderstorms.

Corresponding author address: Milind Sharma, Department of Earth, Atmospheric, and Planetary Sciences, Purdue University, 550 Lafayette St., West Lafayette, IN, 47907; email: sharm261@purdue.edu

a. Charge generation in thunderstorms: microphysics

Several laboratory experiments have successfully reproduced the observed electric fields and charge structures in thunderstorms (Takahashi 1978; Jayaratne et al. 1983; Baker et al. 1987; Baker and Dash 1989). It has been shown through observational and modelling studies that graupel and ice crystals are the two main hydrometeor species participating in the electrification and charge transfer mechanism (Dye et al. 1988; Ziegler et al. 1991; Bruning et al. 2007). In their studies of ice particle interactions, Latham and Mason (1962); Takahashi (1978) found that these ice phase hydrometeors can get charged through collisions even in the absence of an external electric field. This charging mechanism, also known as 'noninductive charging', is capable of producing the observed electric fields within five minutes (Takahashi 1978).

The exact microphysical processes responsible for charge transfer are still relatively less understood, but laboratory studies have found that a quasi-liquid layer facilitates the transfer of mass and thus charge between ice crystals and graupel particles (Baker and Dash 1994). The particle growing at a faster rate from vapor diffusion at the time of collision gets positively charged as per the relative diffusional growth rate theory (Dash et al. (2001); Mitzeva et al. (2005)). However, studies have found that ambient environmental thermodynamics and supercooled liquid water concentration (SCLW) play a crucial role in determining the overall charge polarity to hydrometeors in different regions of a thunderstorm (Berdeklis and List (2001); Saunders (2008); Emersic and Saunders (2010)). Fig. 1 shows the one of the possible relations between SCLW and temperature and the associated variability in polarity of charge transfer to graupel particles as obtained from laboratory experiments (Saunders et al. 2006).

b. Lightning characteristics of supercell thunderstorms

A strong and sustained updraft in a supercell thunderstorm can loft the hydrometeors to higher altitudes (colder

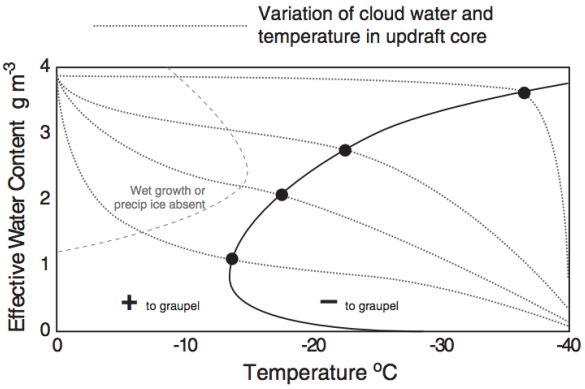

FIG. 1. Illustration of the charge reversal line, depicting the variation in polarity of charge transfer to graupel particles from collisions with ice crystals. Dotted black lines represent liquid water depletion rates in the updraft region. Note the presence of a deeper positively charged region at slow depletion rates. Figure from Bruning et al. (2014).

temperatures) thereby leading to negatively charged graupel particles. However, dry air entrainment may also lead to rapid depletion of available liquid water content (LWC) eventually charging graupel particles with positive polarity. Warm cloud depth also affects the availability of LWC as collision and coalescence processes might reduce the SCLW concentration to low values and therefore, positive charging of graupel particles. Thus, electrification and resulting charge separation is also a dynamic property of thunderstorms.

There have been numerous attempts to explain the intensification of thunderstorms using just lightning data. Supercell thunderstorms and associated tornadic activity were studied by MacGorman et al. (1989) where they found that while ground flash rates had no obvious relationship with the time of tornadoes, the stroke rate in storms was greatest after the tornadic stage ended. They hypothesized that as the updraft intensifies, it elevates the main negative charge region, and thus the distance between the opposite polarity charge regions decreases. This proximity leads to higher frequency of intra-cloud (IC) flashes while the cloud-to-ground (CG) flash rates decrease. On the other hand, when an updraft weakens, the CG flash rates increase as the lower negative charge region descends. However, there is no consensus on the exact mechanism causing variations in the observed IC or CG flash rates. Mansell et al. (2002), through their model simulations, showed that the occurrence of CG flashes depends on the presence of a charge region below the main dipole charge structure (i.e. lowermost layer of positive charge for -CG flashes and negative charge for +CG flashes).

Lang and Rutledge (2002) studied the relationships between storm kinematics, microphysics, and lightning properties of 11 convective storms with varying intensities. They used a combination of peak vertical velocity, volume occupied by significant updrafts within the mixed phase region, and mass flux in the mixed phase region as three indicators for the kinematic intensity of these storms. A comparative analysis revealed that storms with predominantly positive cloud-to-ground (PPCG) flashes featured much larger volumes of significant updrafts (at velocity thresholds of both 10 and 20 m s-1). They further hypothesized that intensification of updrafts leads to higher positive charge production which upon subsequent sedimentation and separation from negative charge region increases the positive CG flash rates.

c. Flash size and rates

Both Bruning and MacGorman (2013); Calhoun et al. (2013) postulated that the charge structure reveals the kinematical structure of a storm as well. They found that the flash rates were much higher where the flash extent had low values. The smallest flash extents were found to exist within the turbulent core updraft regions of thunderstorms. Thus, the inverse relationship between flash rate and extent serves as a good indicator of kinematic texture of storm updrafts. Additionally, Schultz et al. (2015) found that thunderstorms produce a characteristic 'lightning jump' signature while undergoing intensification. This feature was found to be present in storms of varying levels of intensity ranging from weak or ordinary storms to well-organized supercell storms. These findings highlight the combined roles of microphysical and kinematic processes in producing such rapid fluctuations in flash rates in storms.

The main objective of this study is to better understand the relationship between the evolution of cloud microphysics and thunderstorm charge structure. We aim to improve our fundamental understanding of the complex relationship between the storm scale dynamics, cloud physics, and environmental variability and their effect on eventual lightning characteristics of a supercell thunderstorm. We focus on the 19 May 2013 Edmond, Oklahoma cyclic tornadic supercell (refer Wienhoff (2016) for details on synoptic overview) , which produced at least four tornadoes, and peak flash rates of up to 200 flashes per minute.

2. Instrumentation and data processing

a. Lightning mapping array

Lightning source data for this research were collected using the Oklahoma Lightning Mapping Array (OKLMA) network. A total of 15 sensors were active for the duration of interest (2030 UTC till 2230 UTC). These sensors detect the three-dimensional structure of a lightning flash (in the 60-66 MHz VHF band) as the lightning channel emits impulsive radiation during propagation. The nominal range of the OKLMA network is 100 km for three-dimensional and 200 km for two-dimentional (plan) location mapping of flash sources. These sources are mapped

based on the time of arrival (TOA) (see Thomas et al. (2004) for a detailed explanation). The charge structure is inferred based on the bidirectional leader model proposed by Kasemir (1960) and described in MacGorman et al. (2008). According to this model, the negative breakdown leader propagates through positive charge and the positive breakdown leader propagates through negative charge region. Since LMA detects the radiation sources from negative leaders much better than the positive leaders (Thomas et al. 2001), overall detection of the positive charge region is relatively easier. Post-processing of LMA data was performed using the lmatools python package developed by co-author Bruning (`https://github.com/deeplycloudy/lmatools`). The CG lightning data used in this study were from the National Lightning Detection Network (NLDN) which consists of over 100 sensors across the United States Orville (2008). Flashes having a peak current value between -10 kA and +10 kA were removed from the dataset prior to analysis. Such low peak current flash reports are generally IC flashes misreported as CG flashes in the data.

b. KOUN radar

Polarimetric radar variables such as differential reflectivity can compensate the lack of direct measurements of thunderstorm updraft speeds or intensity. The KOUN radar located near Norman, Oklahoma is the original prototype for the Weather Surveillance Radar-1988 Doppler (WSR-88D) and has since been upgraded to polarimetric capabilities. Since KOUN is a research radar, the scan strategy (number and elevation steps) is usually dependent on the purpose of specific case study. For this case, each volume scan consisted of 10 tilts for plan position indicators (PPIs) ranging from elevation angles of 0.5° to 10°. The radar data were objectively analyzed using a Barnes one-pass filter interpolation technique (Barnes 1964).

3. Results

a. Charge analysis

To obtain the net charge structure of the Edmond-Carney supercell, manual charge classification was performed using XLMA software (Thomas et al. 2004) for the period 2130-2150 UTC. Fig. 2 shows an example of such a classification for 2130-2140 UTC, revealing a negative dipole (i.e. upper negative charge above middle level positive charge) structure. The peak source density for negative and positive charge regions occurred around 11 km and 8.5 km respectively. Most of the IC flashes contributing to this anomalous charge structure were classified as inverted ICs (i.e. IC flashes originating between upper level inverted dipole structure. See Bruning et al. (2014) for more details).

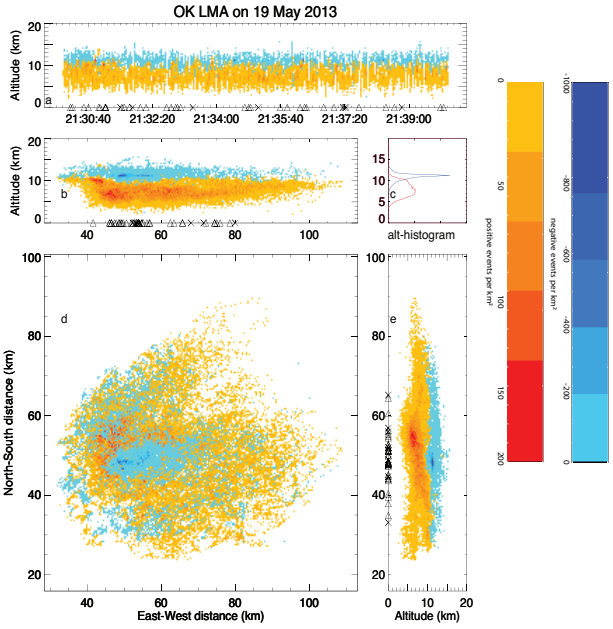

FIG. 2. Manual charge classification performed for the 19 May 2013 Edmond supercell for the period 2130 to 2140 UTC. The sources are color-coded by inferred ambient charge to highlight the vertical dipole structure, with color shading denoting charge density (blue and orange shades for negative and positive charge respectively). Panels show (a) time-height plot of VHF sources, (b) VHF sources projected on an east-west-oriented plane, (c) a histogram of VHF sources, showing distinct peaks for negative (blue) and positive (red) charge regions, (d) plan projection view of all the VHF sources , (e) VHF sources projected on a north-south-oriented plane.

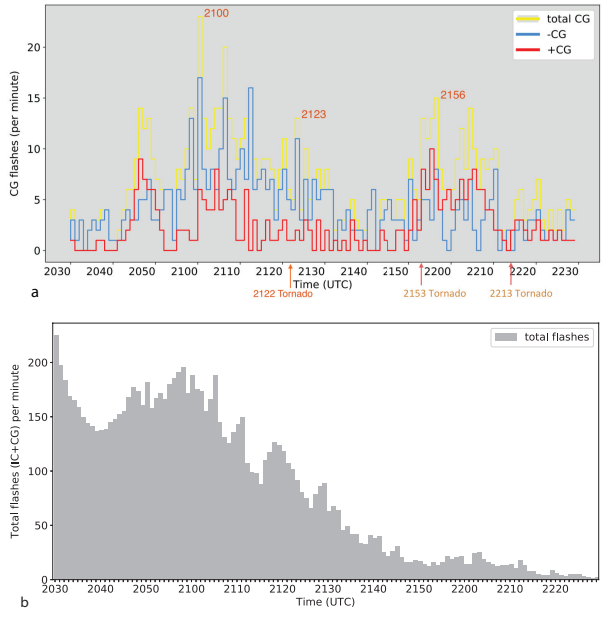

FIG. 3. (a) NLDN-derived CG flash rates (in flashes min^{-1}) in the Edmond-Carney storm, with three times of tornadogenesis, as per National Weather Service (NWS) records (`https://nwschat.weather.gov/lsr/#OUN/201305191800/201305201200/0101`), marked. (b) OKLMA-derived total (IC+CG) flash rates (in flashes min^{-1}).

b. Flash rates

Since there were multiple isolated supercell thunderstorms over central Oklahoma on the day of interest therefore, a "lasso" analysis technique was used to obtain flash rates as a function of height and time from Edmond supercell only (Fig. 3). It is clear that CG flash rates alone are not a good predictor tornadogenesis. Although CG flash rates were high close to the times of the first two tornadogenesis events (2122 and 2153 UTC, respectively), a minimum in CG flash rates was observed around the genesis of the third tornado (2213 UTC). This finding is similar to many such previous observations supporting non-significant correlation between tornadogenesis and CG flash rates (Schultz et al. 2011; Calhoun et al. 2013). Surprisingly, the -CG/+CG ratio was approximately 1.732 for the entire two hour duration of our analysis (i.e. 2030 - 2230 UTC) which is a little higher than the observed ratios in the past (Marshall and Stolzenburg 2002; Krehbiel et al. 2008), but this deviation might be due to the threshold of $\pm$ 10 kA used in our analysis. A sensitivity analysis of the peak current threshold and its effect on the -CG/+CG ratio would be helpful in future.

c. Time-altitude variation of source density

Fig. 4 shows the evolution as a function of time and height of the LMA source density. The portion on figure circled in red, between 2106 and 2117 UTC, denotes a portion of the time series in which the maximum source density temporarily decreased, then rebounded afterward. A tornado developed at 2122 UTC, approximately five minutes after this temporary reduction in maximum source density altitude. We hypothesize that this behavior is directly linked to storm kinematics; it warrants further investigation.

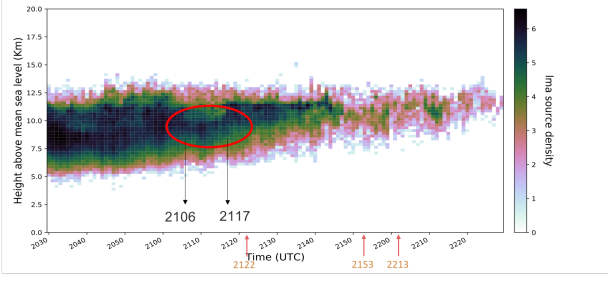

FIG. 4. Time-height plot of the logarithm of VHF source density from OKLMA. Densities are calculated by counting the number of sources that fell into a 0.5 $\times$ 0.5 $\times$ 0.25 km^3 grid volume. Note the upward trend in maximum source density altitude (circled in red) between 2106 and 2117 UTC, prior to the genesis of a tornado at 2122 UTC (indicated on the time axis).

d. Z_{DR} column analysis

As has been discussed in the previous sections, updraft intensification can influence charge gradients and eventual flash rates therefore, we need information on vertical velocity in order to explain the variations in altitude of source density. Kumjian et al. (2014) demonstrated that a Z_{DR} column can be used as a reliable proxy for the strength of a core updraft region in a thunderstorm. A Z_{DR} column is a narrow columnar enhancement of differential reflectivity (Z_DR) extending above the freezing level, typically found in convective storms. Z_{DR} columns are located at the periphery of the updraft maximum in supercells and form as a result of upward lofting of small supercooled rain drops above freezing level. The transition of supercooled liquid water to frozen hydrometeors leads to glaciation of clouds. Differential sedimentation of ice crystals and graupel particles in the mixed phase region leads to rebounding collsions and separation of charges in the clouds. A series of vertical cross-sections through the Edmond-Carney supercell's primary Z_{DR} column (Fig. 5) shows the intensification and vertical growth of the column (panels a-d) in the period corresponding to the relative minimum in source density maxima altitude (2106 - 2117 UTC). This conforms with our hypothesis that an intensifying updraft lofted the hydrometeors at upper levels and led to glaciation of clouds which eventually resulted in flash activity at higher altitudes. Additionally, the Z_{DR} column decayed in altitude at 2121 UTC, approximately two minutes prior to tornadogenesis. A possibile explanation for this observation might be the increased downward-directed pressure perturbation gradient force as the low-level mesocyclone strengthens (Brandes 1978; Trapp 1999). This supports the observational analysis by Picca and Ryzhkov (2015) wherein they proposed the utility of Z_{DR} columns to predict near-term trends in storm intensity.

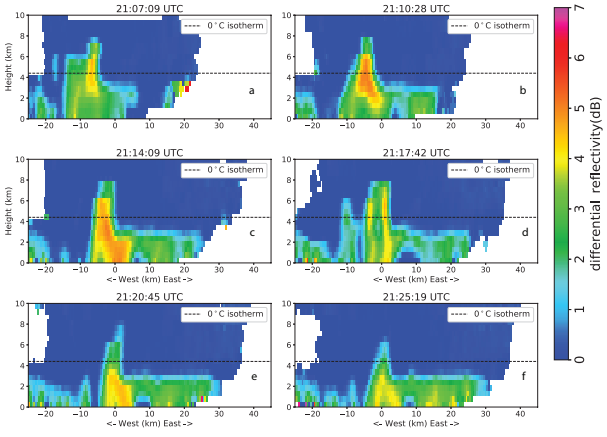

FIG. 5. Evolution of the Edmond-Carney supercell's primary Z_{DR} column, showing north-south vertical cross sections of Z_{DR} (in dB) at (a) 2107 UTC, (b) 2110 UTC, (c) 2114 UTC, (d) 2117 UTC, (e) 2121 UTC, and (f) 2125 UTC. The first four panels (a-d) correspond to the period in which the altitude of maximum source density attained a temporary minium (Fig. 4). Panels (e) and (f) show the collapse of the Z_{DR} column around the time of first tornadogenesis report (2122 UTC).

4. Conclusions

Preliminary results from our analysis of the Edmond supercell reveal interesting relationships between kinematics, microphysics, and the electrification of the storm. The main findings from our current analysis are:

- The Edmond supercell had an anomalous charge structure, with a higher proportion of negative CG flashes with respect to total CG flashes. This is surprising as the ratio of negative CG flashes was high even during the updraft intensification. Since the negative charge existed at the upper levels therefore, we suspect that the dipole might have been tilted to cause higher number of negative CGs. However, a sensitivity analysis for filtering the NLDN data might be needed to avoid inclusion of ICs misclassified as -CGs in the data set.
- There was no direct correlation between CG flash rates and times of tornadogenesis. While CG flash rate peaked around the time of two reports of tornadogenesis (2122 and 2156 UTC), there was a local minimum in the flash rates around the time of third report (2213 UTC). This finding is in accordance with previous attempts at comparison of flash rates with tornadogenesis (Schultz et al. 2011; Calhoun et al. 2013).
- Intensification and vertical growth of the Edmond storm's primary Z_{DR} column correlates well with the altitude of maximum flash activity. Therefore, as expected, Z_{DR} column acts as a good proxy for updrafts in the thunderstorms.

We plan to continue this preliminary work while examining the temporal evolution of flash initiation and source density altitudes with respect to polarimetric variables like correlation coefficient. Additionally, a detailed analysis of the temporal evolution of charge structure within just the Z_{DR} column region can improve our understanding about the effects of kinematic intensity on the complex charge structure. Finally, it will be worthwhile to investigate the contribution of small flashes (< 4 km in size) to the total flash rate. Such a diagnosis will be easier to compare with previous studies and will help explain anomalies, if any exist.

Acknowledgments. This research was supported by National Science Foundation Grant AGS-1741003. Radar data were converted from W2 format to Cf/radial netcdf format by Dr. Jeff Snyder using Warning Decision Support System - Integrated Information (Lakshmanan et al. (2007); `http://www.wdssii.org/`) software. Objective analysis was performed using Py-ART (Helmus and Collis (2016); `http://arm-doe.github.io/pyart/`).

References

Baker, B., M. Baker, E. Jayaratne, J. Latham, and C. Saunders, 1987: The influence of diffusional growth rates on the charge transfer accompanying rebounding collisions between ice crystals and soft hailstones. *Quarterly Journal of the Royal Meteorological Society*, **113 (478)**, 1193–1215.

Baker, M., and J. Dash, 1989: Charge transfer in thunderstorms and the surface melting of ice. *Journal of Crystal Growth*, **97 (3-4)**, 770–776.

Baker, M., and J. Dash, 1994: Mechanism of charge transfer between colliding ice particles in thunderstorms. *Journal of Geophysical Research: Atmospheres*, **99 (D5)**, 10 621–10 626.

Barnes, S. L., 1964: A technique for maximizing details in numerical weather map analysis. *Journal of Applied Meteorology*, **3 (4)**, 396–409.

Berdeklis, P., and R. List, 2001: The ice crystal–graupel collision charging mechanism of thunderstorm electrification. *Journal of the atmospheric sciences*, **58 (18)**, 2751–2770.

Brandes, E. A., 1978: Mesocyclone evolution and tornadogenesis: Some observations. *Monthly Weather Review*, **106 (7)**, 995–1011.

Bruning, E. C., and D. R. MacGorman, 2013: Theory and observations of controls on lightning flash size spectra. *Journal of the Atmospheric Sciences*, **70 (12)**, 4012–4029.

Bruning, E. C., W. D. Rust, D. R. MacGorman, M. I. Biggerstaff, and T. J. Schuur, 2010: Formation of charge structures in a supercell. *Monthly Weather Review*, **138 (10)**, 3740–3761.

Bruning, E. C., W. D. Rust, T. J. Schuur, D. R. MacGorman, P. R. Krehbiel, and W. Rison, 2007: Electrical and polarimetric radar observations of a multicell storm in telex. *Monthly weather review*, **135 (7)**, 2525–2544.

Bruning, E. C., S. A. Weiss, and K. M. Calhoun, 2014: Continuous variability in thunderstorm primary electrification and an evaluation of inverted-polarity terminology. *Atmospheric research*, **135**, 274–284.

Calhoun, K. M., D. R. MacGorman, C. L. Ziegler, and M. I. Biggerstaff, 2013: Evolution of lightning activity and storm charge relative to dual-doppler analysis of a high-precipitation supercell storm. *Monthly Weather Review*, **141 (7)**, 2199–2223.

Calhoun, K. M., E. R. Mansell, D. R. MacGorman, and D. C. Dowell, 2014: Numerical simulations of lightning and storm charge of the 29–30 may 2004 geary, oklahoma, supercell thunderstorm using enkf mobile radar data assimilation. *Monthly Weather Review*, **142 (11)**, 3977–3997.

Dash, J., B. Mason, and J. Wettlaufer, 2001: Theory of charge and mass transfer in ice-ice collisions. *Journal of Geophysical Research: Atmospheres*, **106 (D17)**, 20 395–20 402.

Deierling, W., and W. A. Petersen, 2008: Total lightning activity as an indicator of updraft characteristics. *Journal of Geophysical Research: Atmospheres*, **113 (D16)**.

Dye, J., J. Jones, A. Weinheimer, and W. Winn, 1988: Observations within two regions of charge during initial thunderstorm electrification. *Quarterly Journal of the Royal Meteorological Society*, **114 (483)**, 1271–1290.

Emersic, C., P. Heinselman, D. MacGorman, and E. Bruning, 2011: Lightning activity in a hail-producing storm observed with phased-array radar. *Monthly Weather Review*, **139 (6)**, 1809–1825.

Emersic, C., and C. Saunders, 2010: Further laboratory investigations into the relative diffusional growth rate theory of thunderstorm electrification. *Atmospheric Research*, **98 (2-4)**, 327–340.

Helmus, J. J., and S. M. Collis, 2016: The python arm radar toolkit (py-art), a library for working with weather radar data in the python programming language. *Journal of Open Research Software*, **4**.

Jayaratne, E., C. Saunders, and J. Hallett, 1983: Laboratory studies of the charging of soft-hail during ice crystal interactions. *Quarterly Journal of the Royal Meteorological Society*, **109 (461)**, 609–630.

Kasemir, H. W., 1960: A contribution to the electrostatic theory of a lightning discharge. *Journal of Geophysical Research*, **65 (7)**, 1873–1878.

Krehbiel, P. R., J. A. Riousset, V. P. Pasko, R. J. Thomas, W. Rison, M. A. Stanley, and H. E. Edens, 2008: Upward electrical discharges from thunderstorms. *Nature Geoscience*, **1 (4)**, 233.

Kumjian, M. R., A. P. Khain, N. Benmoshe, E. Ilotoviz, A. V. Ryzhkov, and V. T. Phillips, 2014: The anatomy and physics of z dr columns: Investigating a polarimetric radar signature with a spectral bin microphysical model. *Journal of Applied Meteorology and Climatology*, **53 (7)**, 1820–1843.

Lakshmanan, V., T. Smith, G. Stumpf, and K. Hondl, 2007: The warning decision support system–integrated information. *Weather and Forecasting*, **22 (3)**, 596–612.

Lang, T. J., and S. A. Rutledge, 2002: Relationships between convective storm kinematics, precipitation, and lightning. *Monthly Weather Review*, **130 (10)**, 2492–2506.

Latham, J., and B. J. Mason, 1962: Electrical charging of hail pellets in a polarizing electric held. *Proc. R. Soc. Lond. A*, **266 (1326)**, 387–401.

MacGorman, D. R., D. W. Burgess, V. Mazur, W. D. Rust, W. L. Taylor, and B. C. Johnson, 1989: Lightning rates relative to tornadic storm evolution on 22 may 1981. *Journal of the atmospheric sciences*, **46 (2)**, 221–251.

MacGorman, D. R., and Coauthors, 2008: Telex the thunderstorm electrification and lightning experiment. *Bulletin of the American Meteorological Society*, **89 (7)**, 997–1014.

Mansell, E. R., D. R. MacGorman, C. L. Ziegler, and J. M. Straka, 2002: Simulated three-dimensional branched lightning in a numerical thunderstorm model. *Journal of Geophysical Research: Atmospheres*, **107 (D9)**, ACL–2.

Marshall, T. C., and M. Stolzenburg, 2002: Electrical energy constraints on lightning. *Journal of Geophysical Research: Atmospheres*, **107 (D7)**.

Mitzeva, R., C. Saunders, and B. Tsenova, 2005: A modelling study of the effect of cloud saturation and particle growth rates on charge transfer in thunderstorm electrification. *Atmospheric research*, **76 (1-4)**, 206–221.

Orville, R. E., 2008: Development of the national lightning detection network. *Bulletin of the American Meteorological Society*, **89 (2)**, 180–190.

Picca, S. J. C., Joseph C, and A. V. Ryzhkov, 2015: An observational analysis of z_{DR} column trends in tornadic supercells. *37th Conference on Radar Meteorology, 14 18 September 2015, Norman, Oklahoma*.

Rust, W. D., and D. R. MacGorman, 2002: Possibly inverted-polarity electrical structures in thunderstorms during steps. *Geophysical research letters*, **29 (12)**, 12–1.

Saunders, C., 2008: Charge separation mechanisms in clouds. *Planetary Atmospheric Electricity*, Springer, 335–353.

Saunders, C., H. Bax-Norman, C. Emersic, E. Avila, and N. Castellano, 2006: Laboratory studies of the effect of cloud conditions on graupel/crystal charge transfer in thunderstorm electrification. *Quarterly Journal of the Royal Meteorological Society: A journal of the atmospheric sciences, applied meteorology and physical oceanography*, **132 (621)**, 2653–2673.

Schultz, C. J., L. D. Carey, E. V. Schultz, and R. J. Blakeslee, 2015: Insight into the kinematic and microphysical processes that control lightning jumps. *Weather and Forecasting*, **30 (6)**, 1591–1621.

Schultz, C. J., W. A. Petersen, and L. D. Carey, 2011: Lightning and severe weather: A comparison between total and cloud-to-ground lightning trends. *Weather and forecasting*, **26 (5)**, 744–755.

Stolzenburg, M., W. D. Rust, and T. C. Marshall, 1998a: Electrical structure in thunderstorm convective regions: 2. isolated storms. *Earth's Future*, URL https://agupubs.onlinelibrary.wiley.com/doi/abs/10.1029/97JD03547.

Stolzenburg, M., W. D. Rust, and T. C. Marshall, 1998b: Electrical structure in thunderstorm convective regions: 3. synthesis. *Journal of Geophysical Research: Atmospheres*, **103 (D12)**, 14 09714 108, doi:10.1029/97jd03545.

Stolzenburg, M., W. D. Rust, B. F. Smull, and T. C. Marshall, 1998c: Electrical structure in thunderstorm convective regions: 1. mesoscale convective systems. *Journal of Geophysical Research: Atmospheres*, **103 (D12)**, 14 059–14 078.

Takahashi, T., 1978: Riming electrification as a charge generation mechanism in thunderstorms. *Journal of the Atmospheric Sciences*, **35 (8)**, 1536–1548.

Tessendorf, S. A., S. A. Rutledge, and K. C. Wiens, 2007: Radar and lightning observations of normal and inverted polarity multicellular storms from steps. *Monthly Weather Review*, **135 (11)**, 3682–3706.

Thomas, R. J., P. R. Krehbiel, W. Rison, T. Hamlin, J. Harlin, and D. Shown, 2001: Observations of vhf source powers radiated by lightning. *Geophysical research letters*, **28 (1)**, 143–146.

Thomas, R. J., P. R. Krehbiel, W. Rison, S. J. Hunyady, W. P. Winn, T. Hamlin, and J. Harlin, 2004: Accuracy of the lightning mapping array. *Journal of Geophysical Research: Atmospheres*, **109 (D14)**.

Trapp, R., 1999: Observations of nontornadic low-level mesocyclones and attendant tornadogenesis failure during vortex. *Monthly weather review*, **127 (7)**, 1693–1705.

Wienhoff, Z., 2016: Doppler Radar Analyses of Tornadic Supercells on 19 May 2013. M.S. thesis, University of Oklahoma, Norman, Oklahoma.

Wiens, K. C., T. Hamlin, J. Harlin, and D. M. Suszcynsky, 2008: Relationships among narrow bipolar events,total lightning, and radar-inferred convective strength in great plains thunderstorms. *Journal of Geophysical Research: Atmospheres*, **113 (D5)**.

Williams, E. R., 1989: The tripole structure of thunderstorms. *Journal of Geophysical Research: Atmospheres*, **94 (D11)**, 13 151–13 167.

Ziegler, C. L., D. R. MacGorman, J. E. Dye, and P. S. Ray, 1991: A model evaluation of noninductive graupel-ice charging in the early electrification of a mountain thunderstorm. *Journal of Geophysical Research: Atmospheres*, **96 (D7)**, 12 833–12 855.